Acta Materialia 121 (2016) 202–214

Contents lists available at ScienceDirect

Acta Materialia

journal homepage: www.elsevier.com/locate/actamat

Full length article

Multiple mechanisms of lath martensite plasticity

L. Morsdorf [a], O. Jeannin [a], D. Barbier [b], M. Mitsuhara [c], D. Raabe [a], C.C. Tasan [d, *]

[a] Max-Planck-Institut für Eisenforschung, Max-Planck-Straße 1, 40237 Düsseldorf, Germany
[b] ArcelorMittal Research and Development, Voie Romaine-BP30320, 57283 Maizières-lès-Metz, Cedex, France
[c] Department of Engineering Sciences for Electronics and Materials, Kyushu University, 6-1 Kasugakoen, Kasuga, Fukuoka, 816-8580, Japan
[d] Department of Materials Science and Engineering, Massachusetts Institute of Technology, 77 Massachusetts Avenue, Cambridge, MA 02139, USA

ARTICLE INFO

Article history:
Received 4 July 2016
Received in revised form
2 September 2016
Accepted 5 September 2016

Keywords:
EBSD
Austenite
Micro-mechanics
Strain mapping
DIC

ABSTRACT

The multi-scale complexity of lath martensitic microstructures requires scale-bridging analyses to better understand the deformation mechanisms activated therein. In this study, plasticity in lath martensite is investigated by multi-field mapping of deformation-induced microstructure, topography, and strain evolution at different spatial resolution vs. field-of-view combinations. These investigations reveal site-specific initiation of dislocation activity within laths, as well as significant plastic accommodation in the vicinity of high angle block and packet boundaries. The observation of interface plasticity raises several questions regarding the role of thin inter-lath austenite films. Thus, accompanying transmission electron microscopy and synchrotron x-ray diffraction experiments are carried out to investigate the stability of these films to mechanical loading, and to discuss alternative boundary sliding mechanisms to explain the observed interface strain localization.

1. Introduction

Martensite as a phase is known for its strength and hardness, but not for its ductility. Yet, this crucial constituent of high strength steels does exhibit some level of plastic accommodation, depending on composition [1–5] and thermomechanical treatment history [6–9]. This report aims at extending the current understanding on the micro- and nano-scale deformation mechanisms in lath martensite. The long-term goal of the presented work is to lay foundations for the design of tough, as-quenched lath martensitic steels.

We begin with a brief overview of recent developments in the understanding of lath martensitic structures in steels, since deformation mechanisms are strongly connected to these characteristics. The works of Morito et al. [10,11] and Kitahara et al. [12] introduced the crystallographic hierarchy of lath martensite based on the Kurdjumov-Sachs (K-S) orientation relationship [13] between martensite and prior austenite; $\{110\}_{\alpha'} \parallel \{111\}_{\gamma}$, $\langle 111\rangle_{\alpha'} \parallel \langle 110\rangle_{\gamma}$. The 24 possible variants are grouped into four packets, including six variants sharing the same {110} habit plane, and are further subdivided into blocks separated by high-angle boundaries, sub-blocks and low-misoriented laths. Accordingly, the austenite transforms into thin lath-shaped crystals in between planar interfaces parallel to the $\{110\}_{\alpha'}$ habit plane resulting in a locally anisotropic microstructure, as summarized in Fig. 1. In contrast to equiaxed grains, the extension of laths is restricted in one dimension resulting in a stack of virtually single crystals with thicknesses limited to ~200 nm [14]. The shear deformation involved in martensitic transformation causes a severely dislocated lath structure, which is initially supersaturated with interstitial carbon. Relaxation processes inevitably occur even upon quenching, leading to some degree of (auto-) tempering effects in the as-quenched microstructure [4,15–17].

As a result of these processes and conditions, lath martensitic microstructures exhibit crystallographic, compositional and morphological heterogeneities induced during the course of martensitic transformation from M_s to M_f[15], which are schematically illustrated in Fig. 1. For example, early transforming coarse laths with relatively low dislocation densities (see insets of dislocation networks) are subjected to more extensive auto-tempering during the quenching process (see insets of carbon distribution maps) in comparison to later transforming thinner laths [15]. From a plasticity viewpoint, these heterogeneities (as well as residual stress distribution heterogeneity [9]) should create a scatter in local yield strength even within the bounds of a single prior austenite grain [15,18,19]. Simultaneous presence of several

* Corresponding author.
E-mail address: tasan@mit.edu (C.C. Tasan).

http://dx.doi.org/10.1016/j.actamat.2016.09.006
1359-6454/

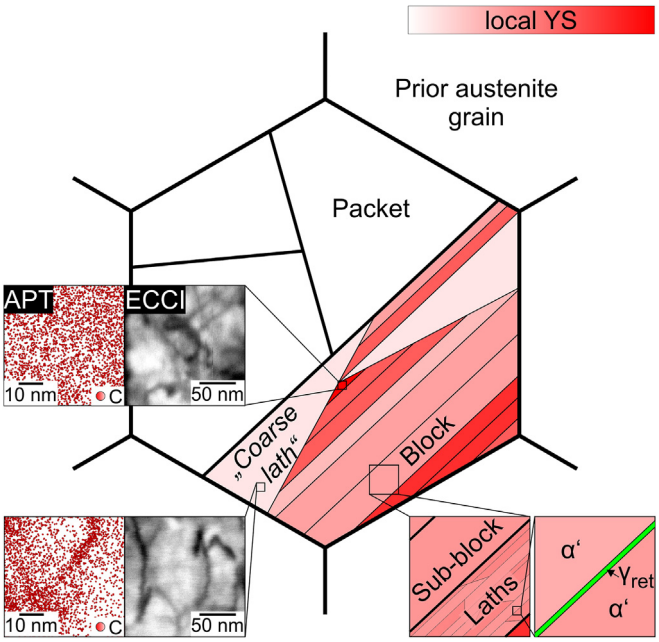

Fig. 1. As-quenched lath martensite microstructure schematically illustrating the crystallographic and topological hierarchy ranging from prior austenite grains to packets, blocks, sub-blocks and laths [10]. Color-code schematically represents possible variations in local yield strength (YS) due to lath size, defect density (see dislocations revealed by electron channeling contrast imaging in the inset) and interstitial carbon content (see atom maps revealed by atom probe tomography analysis in the inset) [15].

further strengthening mechanisms such as solid solution hardening [20] including carbon Cottrell atmosphere effects [21], early stage carbide precipitation [22] and defect interactions [23] explain the martensite's high base strength.

Several studies focused on revealing microstructure-property relationships in lath martensitic steels [24–27]. Since martensite blocks are separated by high angle grain boundaries restricting slip transmission, the effective grain size in martensitic microstructures is usually defined as the block size [24]. This was confirmed by micro-bending tests differentiating low-angle slip transmission and high-angle dislocation pile-up behavior by slip trace analysis [25]. Also, Ghassemi-Armaki et al. found an increase in local strain hardening due to the presence of block boundaries in micro-pillar compression tests [26]. Sub-block boundaries also contribute to boundary strengthening [27].

Considering the bcc slip systems {110}⟨111⟩ and {211}⟨111⟩ [28], together with the geometric lath constraints, leads to the classification of in-lath- and out-of-lath-plane slip. In fact, slip on the {110} habit plane with two possible ⟨111⟩ slip directions intrinsically proceeds parallel to the lath interfaces. The preferential activation of in-lath-plane slip was revealed by in-situ electron backscatter diffraction (EBSD) analyses during tensile deformation by Michiuchi et al. [29], who compared the experimentally observed crystal rotations to predictions by the Sachs- and Taylor model. Nambu et al. described a transition in slip behavior during plastic deformation with first the activation of in-lath-plane slip systems followed by transgranular slip after the transition point, which was observed as a slope change in the true stress-strain curve [30]. Mine et al. subscribed lower critical resolved shear stresses to activate the in-lath-plane slip system as analyzed from micro-tensile tests probing specific morphological and crystallographic orientations in lath martensite [31]. In essence, slip plays an important role in the plastic deformation of low-carbon lath martensite while it is being altered by the morphological and crystallographic constraints given by the hierarchical microstructures.

A number of studies recently showed that the presence of a small fraction of austenite, retained in between martensite laths as thin films even in low-carbon low alloyed steels [32–34] (see Fig. 1), may have an influence in the plasticity of martensite [35–37]. Maresca et al. could reproduce the tensile behavior of lath martensite by incorporating the austenitic phase in crystal plasticity simulations. The results were validated with experimental data from Mine et al. and the model also incorporated the constrained slip activity in lath martensite [36]. Owing to the orientation relationship between martensite and retained austenite, one {111} slip plane in the austenite thin film is intrinsically parallel to the interfacial habit plane, so that the austenite potentially acts as a 'greasy film' in the deformation process [35].

Experimental evidence for this kind of interface plasticity is presently very rare. A recent micro-tensile study by Du et al. revealed sliding of lath martensite substructure boundaries during deformation, which was suggested to be enabled by the presence of thin film retained austenite [38]. On the other hand, Morito et al. found indications for the transformation of retained austenite at low strain levels to similarly oriented fresh martensite by transmission electron microscopy (TEM) analyses [32,39]. Interestingly, Ohmura et al. observed dislocation absorption at a block boundary by in-situ indentation in TEM and suggested a boundary sliding mechanism owing to the {110} nature of martensite interfaces which naturally correspond to the dominant slip plane [40].

The studies suggest that - besides conventional dislocation gliding - interface plasticity requires more attention to completely understand the mechanisms governing lath martensite deformation. The motivation comes not only from the naturally high interface density in martensitic steels, but also from the crystallographically determined character of the different types of interfaces and the presence of a second phase at the interface. With this report we aim at clarifying the occurrence and origin of interface plasticity and its interaction with slip processes in the interface-free martensitic zones and the effect of initial microstructure heterogeneity on these deformation mechanisms.

2. Experimental

Two model low-carbon alloys with compositions Fe-0.13C-5.1Ni and Fe-0.30C-5Ni (wt%) were provided by ArcelorMittal Research in Maizières in form of cold-rolled sheet material. The addition of ~5 wt% Ni promotes enhanced ductility to facilitate the investigation of martensite plasticity. The macroscopic tensile properties in terms of yield strength, tensile strength and elongation to failure are 949 MPa ± 29 MPa, 1239 MPa ± 19 MPa, 13.2% ± 0.4% for Fe-0.13C-5.1Ni and 1308 MPa ± 28 MPa, 1886 MPa ± 49 MPa, 7.5% for Fe-0.30C-5Ni. Lath martensitic microstructures were obtained by austenitization treatment for 5 min at 900°C and subsequent water-quenching. Samples for tensile and bending tests were cut and subjected to a metallographic preparation routine including grinding and polishing in order to allow for surface observations. Three sample surface conditions were used for the subsequent characterization tests. One set of tensile samples was etched in 1% Nital; another set was decorated with a single layer of SiO_2 particles [41]; and the bending sample was used in the as-polished condition. These surface conditions enable a multi-scale characterization approach of the bulk martensite deformation response with large field-of-view strain mapping, high resolution strain mapping and trace analysis, respectively. The combination of strain mapping with topographic surface observations allows analyzing both, the in-plane and out-of-plane strain components on the sample surface.

Fig. 2 shows these surface states respectively (see the insets), and the applied stepwise deformation procedure imposed using a